Letter

# Cellular gradient flow structure linking single-cell-level rules and population-level dynamics

Shuhei A. Horiguchi and Tetsuya J. Kobayashi*
*Graduate School of Information Science and Technology, The University of Tokyo, 7-3-1 Hongo, Bunkyo-ku, Tokyo 113-8656, Japan*

(Received 26 May 2022; accepted 11 May 2023; published 8 June 2023)

In multicellular systems, single-cell behaviors should be coordinated consistently with the overall population dynamics and functions. However, the interrelation between single-cell rules and the population-level goal is still elusive. In this work, we reveal that these two levels are naturally connected via a gradient flow structure of heterogeneous cellular populations and that biologically prevalent single-cell rules, such as unidirectional type switching and hierarchical order in types, emerge from this structure. We also demonstrate the gradient flow structure in a standard model of the T-cell immune response. This theoretical framework works as a basis for understanding multicellular dynamics and functions.

DOI: 10.1103/PhysRevResearch.5.L022052

## I. INTRODUCTION

Multicellular systems are organized dynamically and robustly to shape various populational patterns required to achieve biological functions [1–3]. Because the population dynamics are realized by single-cell-level processes, i.e., cellular proliferation, death, migration, and differentiation, behaviors of individual cells should be coordinated consistently with the overall population dynamics, which may rule the single-cell processes.

For example, phenotypic switching and differentiation of a cell in a population are often unidirectional. Moreover, the multiple cell types are hierarchically ordered, and their kinetic properties, e.g., type-switching and proliferation rates, also seem to be coupled. The existence of hierarchy, or equivalently, acyclic cell-type lineage structures and kinetic coupling are prevalent in multicellular systems from immunity to development [4–7]. These single-cell rules emerging in a population may be related to the functions and the coordination of the population.

The notion of the epigenetic landscape has been used pervasively to describe the robust and directional dynamics among hierarchical cellular types, where individual cells are likened to balls rolling down the landscape [8–10]. However, populationally coordinated behaviors cannot be achieved merely by the independent dynamics of individual cells following the landscape. The individual landscapes should be modulated by the dynamics of the other cells in the population to attain functional and robust trajectories at the population level. Thus, not the individual cells but the population itself follows the landscape characterizing the biological function. Yet individual cells also seem to follow their own landscapes. This entangled relation between landscapes for the whole population and individuals has rarely been appreciated and investigated [11–13].

In this work, we show that the interrelation between single-cell and population levels can naturally emerge from a gradient flow structure of a population. We model the desirable population distribution for achieving a biological function by the landscape of a biological utility function. Then, we derive the population dynamics that maximize the utility given the biological costs of single-cell processes, which results in a gradient flow of the utility function. We demonstrate as an example that the standard model of T-cell population dynamics in the acute immune response [14] can be understood as the gradient flow. From the populational gradient flow structure, the single-cell-level landscape emerges, from which the unidirectional type switching, hierarchical cell type, and kinetic couplings are generally derived. Moreover, the single-cell landscape is related to the population-level utility landscape as its functional variation. Our result can work as a theoretical basis to bridge single-cell-level rules and behaviors with population-level dynamics and functions of multicellular systems.

## II. GRADIENT FLOW OF CELLULAR POPULATION DYNAMICS

We first introduce the governing equations of the heterogeneous cellular population dynamics. We consider a large heterogeneous population of cells with different types. The state of population at time $t$ is characterized by $n_t = \{n_t(x)\}_{x\in X}$, where $n_t(x) \geqslant 0$ is the population size of the cells with type $x \in X$. Here $X$ is a set of all possible types. The state of the population changes over time by the following cellular actions: growth (proliferation minus death), type switching, and immigration (recruitment) of new cells from outside of the population. Their rates are assumed to be type dependent

*Also at Institute of Industrial Science, The University of Tokyo, 4-6-1 Komaba Meguro-ku, Tokyo 153-8505, Japan; tetsuya@mail.crmind.net

*Published by the American Physical Society under the terms of the Creative Commons Attribution 4.0 International license. Further distribution of this work must maintain attribution to the author(s) and the published article's title, journal citation, and DOI.*

such that $g_t(x)$ is the growth rate of type $x$, $v_t(x, y) \geqslant 0$ is the type-switching rate from type $x$ to type $y$, and $m_t(x) \geqslant 0$ is the immigration rate of type $x$. In this work, we focus on the case where $X$ is discrete, but it can be easily extended to the continuum case. Then, the population dynamics of the cells can be described by the following equations:

$$\begin{aligned}\frac{dn_t(x)}{dt} &= n_t(x)g_t(x) + m_t(x) \\ &\quad - \sum_{y\in X}[n_t(x)v_t(x, y) - n_t(y)v_t(y, x)] \\ &=: F_x(n, g, m, v), \end{aligned} \tag{1}$$

where we approximate $n_t(x)$ as a continuous variable, which is valid if the population size is large enough. While we treat the types as phenotypic states in this work, they can be treated more generally to include any features of a cell such as position or niche where it resides. For such a case, type switching is understood as the migration of cells among different spatial compartments in a metapopulation.

Next, we connect the population dynamics with biological functions. To this end, we introduce a *utility function* $U_t(n)$. The utility function $U_t(n)$ abstractly represents how good a given population distribution $n$ is under the situation at time $t$. The time dependence of $U_t(n)$ is essential for modeling various biological situations. For example, if a pathogen invades our body, a particular population distribution $n$ of immune cells would work more effectively than another $n'$, which is represented as $U_t(n) > U_t(n')$. The utility may change after the eviction of the pathogen, which is captured by the time dependence of $U_t(n)$. Therefore, the dynamics that can induce the population distribution $n_t(x)$ into the one with a higher utility more promptly would be more functional than other dynamics.

However, the rates of growth, immigration, and type switching cannot be arbitrarily high due to the biological cost of those processes and physical constraints. In order to account for it, we introduce the *cost function* $C_n(g, m, v)$. The cost function abstractly characterizes the instantaneous biological cost of taking cellular actions at given rates $(g, m, v)$, which is nonnegative and dependent on the current population $n$. In this work, we consider the cost function to have the following form:

$$\begin{aligned} C_n(g, m, v) &= \frac{1}{2}\sum_{x\in X} n(x)w_g(x)g(x)^2 \\ &\quad + \frac{1}{2}\sum_{x\in X} w_m(x)m(x)^2 \\ &\quad + \frac{1}{2}\sum_{x,y\in X} n(x)w_v(x, y)v(x, y)^2 \geqslant 0, \end{aligned} \tag{2}$$

where $w_g$, $w_m$, and $w_v$ are positive weights whose values depend on the single-cell level mechanisms of actions.

This form of the cost function is derived from three assumptions: (1) costs for different cellular actions are independent, i.e., the total cost is just a sum of them; (2) the growth cost and the type-switching cost are proportional to the current cell number $n(x)$; and (3) for each cellular action, the cost is a convex and superlinear function of the rate. The second assumption is reasonable because growth and type-switching costs are incurred for each cell in the current population. In contrast, since immigration is usually independent of the current population, the immigration cost is not proportional to the current cell number. The third assumption is crucial to prohibit the optimal action rates from being arbitrarily high. Such unrealistic behavior can happen if the cost grows slowly as the rates increase and if the increase in the utility can cancel it out. While we focus here on the quadratic cost function, the simplest convex function, our theory can be extended to more general convex functions. The mathematical background and biological interpretation of the cost function are presented in the Appendix and Secs. B and C of the Supplemental Material [15].

We consider the population dynamics of Eq. (1) where the rates $(g_t, m_t, v_t)$ are determined to maximize the value of the utility function under the cost:

$$\underset{g,m,v}{\text{maximize}}\ U_{t+\Delta t}(n_{t+\Delta t}) - \int_t^{t+\Delta t} C_{n_\tau}(g_\tau, m_\tau, v_\tau)d\tau, \tag{3}$$

subject to the governing equations in Eq. (1). The objective is to maximize the utility at the future time point $t + \Delta t$ while minimizing the cumulative cost from time $t$ to $t + \Delta t$. To simplify the subsequent derivation, we assume that $\Delta t$ is small, yet almost the same conclusions could be obtained without this assumption. In the limit $\Delta t \to 0$, Eq. (3) becomes

$$\underset{g,m,v}{\text{maximize}}\ \text{Diff}_{n_t}U_t(g, m, v) - C_{n_t}(g, m, v), \tag{4}$$

where $\text{Diff}_{n_t}U_t(g, m, v)$ is the time derivative of $U_t$ through the time evolution of $n_t$ given rates $(g, m, v)$:

$$\text{Diff}_{n_t}U_t(g, m, v) := \sum_{x\in X}\frac{\delta U_t(n_t)}{\delta n}(x)F_x(n_t, g, m, v).$$

We could obtain the explicit form of the unique optimum $(g_t^\dagger, m_t^\dagger, v_t^\dagger)$ of the above optimization problem as follows (see Sec. A in the Supplemental Material [15] for the derivation):

$$g_t^\dagger(x) = \frac{1}{w_g(x)}\frac{\delta U_t(n_t)}{\delta n}(x), \tag{5a}$$

$$m_t^\dagger(x) = \frac{1}{w_m(x)}\left[\frac{\delta U_t(n_t)}{\delta n}(x)\right]_+, \tag{5b}$$

$$v_t^\dagger(x, y) = \frac{1}{w_v(x, y)}\left[\overline{\nabla}\frac{\delta U_t(n_t)}{\delta n}(x, y)\right]_+, \tag{5c}$$

where $[a]_+ := \max\{a, 0\}$ is the positive part of $a \in \mathbb{R}$, and $\overline{\nabla}$ is the discrete gradient operator, i.e., for any $\phi : X \to \mathbb{R}$, $\overline{\nabla}\phi(x, y) := \phi(y) - \phi(x)$. Note that these optimum rates are scale invariant: they are invariant under the rescaling of the utility function $U_t$ and the cost function $C$ with the same factor.

Let us consider the dynamics with the optimal rates $(g_t, m_t, v_t) = (g_t^\dagger, m_t^\dagger, v_t^\dagger)$. Under this dynamics, the value of the utility function $U_t(n)$ evolves as

$$\begin{aligned}\frac{d}{dt}[U_t(n_t)] &= \frac{\partial U_t}{\partial t}(n_t) + \text{Diff}_{n_t}U_t(g_t^\dagger, m_t^\dagger, v_t^\dagger) \\ &= \frac{\partial U_t}{\partial t}(n_t) + 2C_{n_t}(g_t^\dagger, m_t^\dagger, v_t^\dagger), \end{aligned} \tag{6}$$

which is also derived in the Supplemental Material. Since the instantaneous cost $C_{n_t}$ is nonnegative, the value of the utility function always increases when $\frac{\partial U_t}{\partial t}$ vanishes. Indeed, when $U_t$ does not depend on $t$, the dynamics is a generalized gradient flow of $U$, where $C$ is considered a dissipation function [16–18].

## III. T-CELL IMMUNE RESPONSE MODEL

We demonstrate that a model of T-cell population dynamics in the acute immune response [14] is a gradient flow in our sense. Here we introduce a slightly modified version of the model proposed in [14]. The model assumes three types of T cells—naive ($N$), activated effector ($A$), and memory ($M$)—and the numbers of these cells $n_t(N)$, $n_t(A)$, and $n_t(M)$ are described by the following ordinary differential equations:

$$\begin{aligned}\frac{dn_t(N)}{dt} &= m_N + g_N n_t(N) - v_{NA} I_t n_t(N),\\ \frac{dn_t(A)}{dt} &= (g_{A0} + g_{A1} I_t) n_t(A) + v_{NA} I_t n_t(N)\\ &\quad + v_{MA} I_t n_t(M) - v_{AM}(1 - I_t) n_t(A),\\ \frac{dn_t(M)}{dt} &= g_M n_t(M) - v_{MA} I_t n_t(M)\\ &\quad + v_{AM}(1 - I_t) n_t(A),\end{aligned} \tag{7}$$

where $g$, $m$, and $v$ are constant growth, immigration, and type-switching rates, and $I_t$ represents the temporal change in the environmental situation such that $I_t = 0$ when the immune cells should contract to recover to the normal state, and $I_t = 1$ when they should expand to eliminate pathogens [Fig. 1(a)]. We assume an on/off transition:

$$I_t = \begin{cases} 1 & \text{if } \tau_0 \leqslant t < \tau_1 \\ 0 & \text{otherwise.} \end{cases} \tag{8}$$

A typical time evolution is depicted in Fig. 1(b). In the expansion phase ($\tau_0 \leqslant t < \tau_1$), the number of activated T cells rapidly increases, whereas, in the contraction phase ($\tau_1 \leqslant t$), the number of memory T cells increases instead.

There are several versions of the T-cell immune response model, and their mathematical properties were investigated in [19–21]. The model we introduced in Eqs. (7) and (8) is simple yet includes immunologically realistic factors. Notably, a simplified version of the model introduced here was shown to reproduce experimental data [14,22]. In Secs. D–G of the Supplemental Material, we list some other T-cell immune response models and discuss their gradient flow structures.

The model of Eqs. (7) and (8) is a gradient flow in our framework on three-type space $X = \{N, A, M\}$ with the following utility function $U_t$ and the cost function $C$. The utility function is a time-dependent linear function

$$U_t(n) = u_N n(N) + u_A^{(I_t)} n(A) + u_M n(M), \tag{9}$$

with coefficients $u_N := g_N \rho_N w_0$, $u_A^{(I_t)} := (g_{A0} + g_{A1} I_t) w_0$, and $u_M := g_M \rho_M w_0$, indicating that each cell type has different importance depending on the environmental situation. The

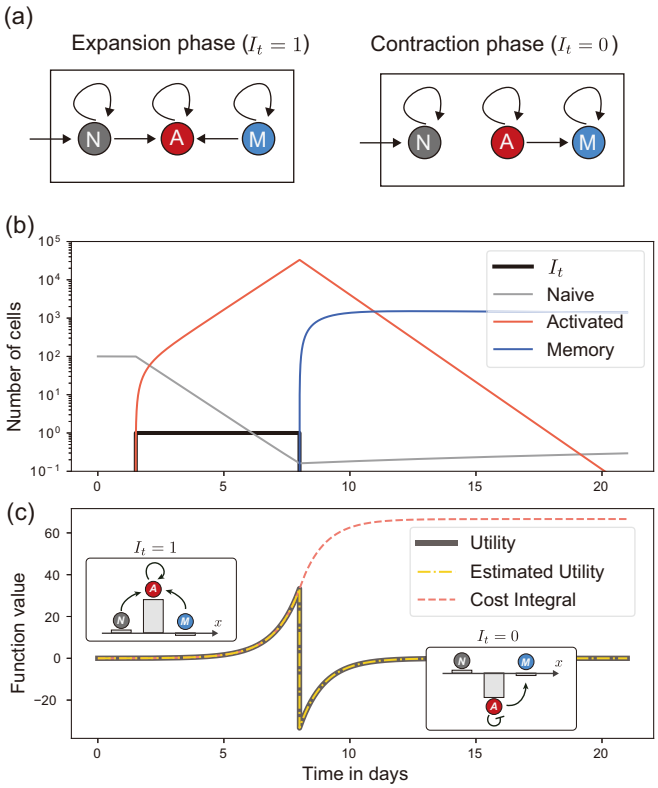


FIG. 1. (a) Schematic illustration of the immune response model with three types: naive ($N$), activated ($A$), and memory ($M$) T cells. (b) Time evolution of the numbers of T cells of the three types. (c) Time evolution of the utility $U_t(n_t)$, the estimated utility based on Eq. (6), and the time integral of the cost $2\int_0^t C_{n_\tau}(g_\tau^\dagger, m_\tau^\dagger, v_\tau^\dagger)d\tau$. A sketch of single-cell-level utility landscapes $u_t(x) = \frac{\delta U_t(n_t)}{\delta n}(x)$ is also shown in the inset. The parameters are $m_N = 0.01$, $g_N = 0.001$, $g_{A0} = -1$, $g_{A1} = 2$, $g_M = -0.01$, $v_{N,A} = v_{M,A} = 1$, $v_{A,M} = 0.05$ day$^{-1}$, $w_0 = 10^{-3}$, and $\rho_N = \rho_M = 1$. The simulation starts at $t = 0$ with $n_0(N) = 100$, $n_0(A) = n_0(M) = 0$ and the value of $I_t$ switches at time $\tau_0 = 1.5$ and $\tau_1 = 8$ day.

cost function [Eq. (2)] is specified with the weights

$$\begin{aligned} w_g(N) &= \rho_N w_0, \quad w_g(A) = w_0, \quad w_g(M) = \rho_M w_0,\\ w_m(N) &= \frac{u_N}{m_N} = \frac{g_N \rho_N}{m_N} w_0,\\ w_v(N,A) &= \frac{u_A^{(1)} - u_N}{v_{NA}} = \frac{(g_{A0} + g_{A1}) - g_N \rho_N}{v_{NA}} w_0,\\ w_v(M,A) &= \frac{u_A^{(1)} - u_M}{v_{MA}} = \frac{(g_{A0} + g_{A1}) - g_M \rho_M}{v_{MA}} w_0,\\ w_v(A,M) &= \frac{u_M - u_A^{(0)}}{v_{AM}} = \frac{g_M \rho_M - g_{A0}}{v_{AM}} w_0, \end{aligned} \tag{10}$$

and all the other weights are $+\infty$. Here, $w_0$, $\rho_N$, and $\rho_M$ are arbitrary positive constants. By taking account of the scale invariance of the optimal rates, $w_0$ is the scaling factor for the utility function and the cost function. We define it as the same as the growth weight for activated T cells. $\rho_N$ and $\rho_M$ are the relative growth weights for naive and memory T cells.

To demonstrate that the model is actually a gradient flow, we numerically calculated $U_t(n_t)$, the value of utility function

along the time evolution of $n_t$ [Fig. 1(c)]. The result shows that $U_t(n_t)$ is monotonically increasing except at the change point $t = \tau_1$, where $\frac{\partial U_t}{\partial t}$ in Eq. (6) becomes nonzero. Thus, the gradient flow structure completely explains this behavior.

Finally, we discuss that the gradient flow structure is qualitatively consistent with biologically plausible parameters. The structure imposes the positivity of the weights [Eqs. (10)] of the cost function. Rearranging the terms, we obtain the following constraints on the growth rates:

$$0 < g_N < (g_{A0} + g_{A1})\frac{1}{\rho_N},$$
$$g_{A0}\frac{1}{\rho_M} < g_M < (g_{A0} + g_{A1})\frac{1}{\rho_M}. \tag{11}$$

If these inequalities do not hold, the increase in utility is no longer guaranteed. The existence of expansion and contraction in the immune response naturally requires that the growth rate for the activated T cells in the contraction phase is negative ($g_{A0} < 0$) and that the growth rate for the activated T cells in the expansion phase is positive ($g_{A0} + g_{A1} > 0$). If, in addition, the growth rate $g_N$ for the naive T cells is positive, there exist the weight parameters $\rho_N$ and $\rho_M$ satisfying the constraints. According to [23], naive T cells in humans have a relatively high proliferation rate to maintain the size of the naive T-cell population, implying the growth rate $g_N$ for the naive T cells to be positive. Thus, the gradient flow structure is consistent with biologically plausible parameters.

## IV. EMERGING SINGLE-CELL RULES

While our gradient flow is derived from the optimization at the population level, i.e., what kind of populational change is better than others, it also determines the behaviors of each cell, i.e., what a cell of type $x$ should do or should not do. We will show two such rules derived from the gradient flow structure. In both rules, the functional derivative $\frac{\delta U_t(n_t)}{\delta n}(x) := u_t(x)$ of the utility function plays a vital role. One can interpret this function $u_t(x)$ as a utility function at the single-cell level because it defines which type is preferable to the other types. This contrasts with the original utility function $U_t(n)$, which defines a metric only for the population of cells. The relationship of $U_t(n)$ and $u_t(x)$ is also close to that of thermodynamic potential and chemical potential in thermodynamics [24].

In the T-cell immune response model, the single-cell level utility is given by $u_t(N) = u_N = g_N \rho_N w_0$, $u_t(A) = u_A^{(I_t)} = (g_{A0} + g_{A1} I_t) w_0$, and $u_t(M) = u_M = g_M \rho_M w_0$. If the conditions in Eqs. (11) hold, the activated T cell has the highest utility $u_t(A) = (g_{A0} + g_{A1}) w_0 > 0$ in the expansion phase, whereas it has the lowest utility $g_{A0} w_0 < 0$ in the contraction phase [see the inset of Fig. 1(c)].

### A. Unidirectional phenotypic transition

In multicellular systems, unidirectional phenotypic switchings are commonly observed in single-cell-level dynamics, which supports the notion of the epigenetic landscape. For example, the T-cell immune response model does not have bidirectional or cyclic-type switchings. We show that such unidirectionality is tightly linked to the gradient flow structure.

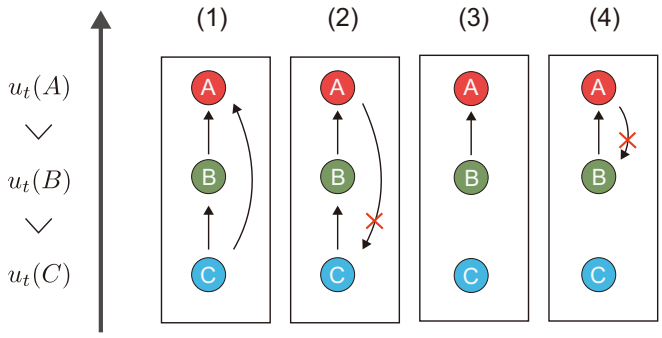


FIG. 2. Examples of type-switching graphs of three types $X = \{A, B, C\}$. While acyclic graphs (1) and (3) are allowed in the gradient flow, graphs (2) and (4) contain a cycle and never appear in the gradient flow. For graphs (2) and (4), the edge with the cross is incompatible with the ordering by $u_t(x) = \frac{\delta U_t(n_t)}{\delta n}(x)$.

To this end, we consider a type-switching graph $G_t$. The nodes of the graph $G_t$ are types $X$, and an edge from type $x$ to $y$ exists if and only if the type-switching rate is not zero, i.e., $v_t^\dagger(x, y) > 0$. One can show that this graph $G_t$ for any gradient flow is always acyclic (Fig. 2). In the simplest case, the types $x$ and $y$ cannot have bidirectional type switching because $v_t^\dagger(x, y)$ and $v_t^\dagger(y, x)$ cannot be simultaneously positive from Eq. (5c). Depending on the sign of $\overline{\nabla} u_t(x, y)$, either or both of $v_t^\dagger(x, y)$ and $v_t^\dagger(y, x)$ is zero. In other words, cells of type $x$ switch to type $y$ if and only if $y$ is better than $x$, which means that

$$u_t(x) < u_t(y). \tag{12}$$

If we place all the types $X$ vertically in the order of $u_t$ as in Fig. 2, every type-switching edge points upward. Thus, more generally, three or more types cannot have any cyclic-type switching. If a cycle exists, at least one of the edges points downward, which contradicts the ordering by $u_t$.

One can view $u_t = \frac{\delta U_t(n_t)}{\delta n}$ as a kind of epigenetic landscape of single cells [8]. We note that it depends on time $t$ and the current population $n_t$, which could be interpreted as fluctuations of the epigenetic landscape due to time-dependent external signals and cell-cell interactions.

We also note that the type-switching graph of a gradient flow may appear to have a cycle if one ignores the time dependence of the graph. Indeed, the type-switching graph of the T-cell immune response model contains a cycle (from activated to memory and from memory to activated) if one lumps the type-switching edges throughout the immune response.

### B. Coupling

Growth, immigration, and phenotypic switching in multicellular systems are not independent. For example, in the T-cell immune response model, the growth and type-switching rates change simultaneously when the environmental condition changes. We show that the gradient flow structure implies cooperative relationships among growth, immigration, and type-switching rates.

Consider the simplest setting where all the weights are finite and constant, $w_g(x) = w_m(x) = w_v(x, y) = 1\ \forall x, y \in X$. From the fact that the growth rates, immigration rates, and

type-switching rates [Eqs. (5)] have the same term $\frac{\delta U_t(n_t)}{\delta n} = u_t$, we find some relations among them. When there is an immigration flux to type $x$, the growth rate of type $x$ must be positive and vice versa:

$$m_t^\dagger(x) > 0 \Leftrightarrow g_t^\dagger(x) > 0. \tag{13}$$

When the type-switching rate from type $x$ to $y$ is positive, the growth rates of the source type $x$ must be lower than the growth rate of the destination type $y$:

$$v_t^\dagger(x, y) > 0 \Leftrightarrow g_t^\dagger(x) < g_t^\dagger(y). \tag{14}$$

One can intuitively understand these effects as cooperation among growth, immigration, and type switching to achieve the same goal: maximizing the utility function.

The T-cell immune response model has this cooperative coupling as long as the inequalities in Eq. (11) are satisfied. The coupling between growth and type switching was also predicted in Furusawa and Kaneko's model: the growth rate of stem-type cells is lower than differentiated-type cells [12]. Moreover, this kind of coupling has been observed in cell biology: cells undergoing differentiation stop the cell cycle and do not divide [7]. Other coupling properties predicted from the gradient flow structure can be used to search for the structure in actual biological systems.

## V. DISCUSSION

In this work, we proposed a theoretical framework that links the functional dynamics of multicellular systems with the individual dynamics of constituent cells. The rules in the single-cell level dynamics were naturally derived and explained from the functionality and coordination of the population from this framework. A standard T-cell immune response model was shown to be consistent with these results. By examining the model, we demonstrated that the framework could identify the crucial characteristics in the single-cell dynamics for the whole populational system to be functional.

While we employed the immune response as an example, the framework may be applied to other multicellular systems and phenomena. However, quantitative models consistent with experiments like Eq. (7) may not always be available. For such a case, the crucial step would be systematic identification or inference of the utility and cost functions from experimentally observed dynamics for a given phenomenon. To this end, our formulation may be combined with techniques in machine learning and single-cell omics to infer the dynamics with potential landscapes [25,26]. We may also derive the cost function from the physical and thermodynamic principles, e.g., by the large deviation theory [18]. In either case, our framework will serve as a basis for linking the single-cell and population properties.

Finally, it should be noted that a given population dynamics may not always fall into the class of gradient flow in the strict sense. Some modifications of the T-cell model [Eqs. (7) and (8)] can violate the conditions to be a gradient flow, e.g., having bidirectional type switching or having negative growth rate and positive immigration rate at the same time. Nevertheless, the gradient-flow-like behaviors can still survive if the modification is moderate, and the utility monotonically increases in time (see Supplemental Material for more details [15]). Our theory can be used to search for such behaviors. Alternatively, we can further extend the notion of gradient flow [27,28] to accommodate oscillatory components, e.g., cell cycle, and others. It expands the applicability of our approach to a wide range of multicellular phenomena and will be pursued.

## ACKNOWLEDGMENTS

We thank Kenji Itao for his helpful comments. S.A.H. is financially supported by the JSPS Research Fellowship Grant No. JP21J21415. This research is supported by JST (Grants No. JPMJCR2011 and No. JPMJCR1927) and JSPS (Grant No. 19H05799).

## APPENDIX: GENERALIZED GRADIENT FLOWS

In this Appendix, we briefly review the generalized gradient flow and explain a geometric interpretation of the cost function in Eq. (2). For details, see Sec. B of the Supplemental Material [15].

Consider the set of cell number distribution of types $X$ as a smooth manifold $\mathcal{M} = \mathbb{R}^{|X|}_{\geqslant 0}$, which is a subset of finite-dimensional linear space. We write $T_n\mathcal{M} \cong \mathbb{R}^{|X|}$ and $T_n^*\mathcal{M} \cong \mathbb{R}^{|X|}$ to stand for the tangent and cotangent spaces at a point $n \in \mathcal{M}$. We denote by $\langle u, v\rangle$ the bilinear product of a cotangent vector $u \in T_n^*\mathcal{M}$ and a tangent vector $v \in T_n\mathcal{M}$.

The gradient flow can be intuitively formulated as the steepest ascent of a differentiable function $U : \mathcal{M} \to \mathbb{R}$. Given $n_t$ at time $t$, we choose $n_{t+\Delta t}$ so that $U(n_{t+\Delta t})$ is as large as possible while the distance $d(n_{t+\Delta t}, n_t)$ should be less than or equal to a given small value $\varepsilon > 0$, i.e., $n_{t+\Delta t}$ is the optimal $n$ of the following optimization problem:

$$\underset{n}{\text{maximize}}\ U(n), \quad \text{such that } \tfrac{1}{2}d(n, n_t)^2 \leqslant \varepsilon.$$

Equivalently, we maximize $U(n_{t+\Delta t})$ with the distance $d(n_{t+\Delta t}, n_t)$ as a penalty:

$$\underset{n}{\text{maximize}}\quad U(n) - \frac{1}{2\Delta t}d(n, n_t)^2. \tag{A1}$$

Taking the limit $\Delta t \to 0$, the optimization provides the continuous-time evolution of $n_t$. Equation (A1) is called a minimizing movement scheme of the gradient flow [16].

Alternatively, we may directly specify the tangent vector $\dot{n} \in T_n\mathcal{M}$ at each point $n \in \mathcal{M}$. Let $\|\cdot\|_n : T_n\mathcal{M} \to [0, \infty)$ be a norm on the tangent space at $n$. The tangent vector is determined to maximize the increase of $U$ while the (squared) length of the tangent vector should be minimized.

$$\underset{\dot{n}}{\text{maximize}}\quad U(n_{t+\Delta t}) - \int_t^{t+\Delta t} \frac{1}{2}\|\dot{n}_\tau\|_{n_\tau}^2 d\tau,$$

where the curve $\{n_\tau\}_{\tau\in[t,t+\Delta t]}$ satisfies $\frac{dn_\tau}{d\tau} = \dot{n}_\tau$ and $n_t = n$. In the limit $\Delta t \to 0$, the above problem becomes

$$\underset{\dot{n}\in T_n\mathcal{M}}{\text{maximize}}\quad \mathrm{Diff}_n U(\dot{n}) - \tfrac{1}{2}\|\dot{n}\|_n^2, \tag{A2}$$

where $\mathrm{Diff}_n U(\dot{n}) := \langle DU(n), \dot{n}\rangle = \frac{d}{dt}U(n_t)|_{n_t=n}$, and $DU \in T_n^*\mathcal{M}$ is the derivative of $U$ with respect to $n$. The solution to this optimization is the optimal tangent vector $\dot{n}^\dagger(n)$ as a

function of $n$, which induces the gradient flow $\frac{dn_t}{dt} = \dot{n}^\dagger(n_t)$, and $U(n_t)$ monotonically increases in time.

In the above formulations, $d$ and $\|\cdot\|_n$ satisfy the axiom of distance and norm. However, we can choose more general functions for $d$ and $\|\cdot\|_n$ that are not necessarily distance or norm. One generalization is, instead of a norm, to use a dissipation function $\Psi_n : T_n\mathcal{M} \to [0, \infty]$ which is nonnegative, strictly convex, differentiable, superlinear, and satisfying $\Psi_n(0) = 0$, for each point $n \in \mathcal{M}$. The optimization problem to determine the tangent vector at $n$ is just replacing $\frac{1}{2}\|\cdot\|_n^2$ in Eq. (A2) with $\Psi_n$,

$$\underset{\dot{n}\in T_n\mathcal{M}}{\text{maximize}} \quad \text{Diff}_n U(\dot{n}) - \Psi_n(\dot{n}).$$

One can show that the optimal solution $\dot{n}^\dagger(n)$ satisfies $\text{Diff}_n U[\dot{n}^\dagger(n)] \geqslant 0$. The conditions on $\Psi_n$ guarantee that the $U(n_t)$ increases in time. This formulation is described in, e.g., [17].

One further generalization is to introduce a linear parametrization of the tangent space. Let $\Theta_n$ be the parameter space at $n \in \mathcal{M}$, and we have a linear mapping $A_n : \Theta_n \to T_n\mathcal{M}$. We define a function $C_n : \Theta_n \to [0, \infty]$ which is nonnegative, strictly convex, differentiable, superlinear, and satisfying $C_n(0) = 0$. For each $n \in \mathcal{M}$, the optimal parameter $\theta^\dagger(n)$ is determined by the following optimization problem:

$$\underset{\theta\in\Theta_n}{\text{maximize}} \quad \text{Diff}_n U(\theta) - C_n(\theta),$$

where $\text{Diff}_n U(\theta) := \text{Diff}_n U(A_n\theta) = \langle DU(n), A_n\theta\rangle$. With the optimal parameter $\theta^\dagger(n)$, the time evolution of $n$ is written by

$$\frac{dn_t}{dt} = A_{n_t}\theta^\dagger(n_t) = A_{n_t}\partial C_n^*\left[A_n^\top DU(n)\right],$$

where $C_n^*$ is the Legendre transform of $C_n$. One can show that $\text{Diff}_n U[\theta^\dagger(n)] \geqslant 0$. This formulation is described in [29].

We use the last formulation to derive the gradient flow for cellular population dynamics. The growth, immigration, and type-switching rates correspond to the parameter $\theta = (g, m, v)$, and the mapping $A_n$ is given by the function $F$ in Eq. (1). Also, the cost function $C_n$ in Eq. (2) satisfies the above conditions. Therefore, the cost function can be interpreted as a normlike function on the tangent space but parametrized with rates $(g, m, v)$.


[1] F. Alenzi, B. Alenazi, M. Salem, A. Al-Jabri, and R. Wyse, The haemopoietic stem cell: Between apoptosis and self renewal, Yale J. Biol. Med. **82**, 7 (2009).

[2] Y. Lee, M. Decker, H. Lee, and L. Ding, Extrinsic regulation of hematopoietic stem cells in development, homeostasis and diseases, WIREs Dev. Biol. **6**, e279 (2017).

[3] G. von Dassow, E. Meir, E. M. Munro, and G. M. Odell, The segment polarity network is a robust developmental module, Nature **406**, 188 (2000).

[4] D. E. Wagner, C. Weinreb, Z. M. Collins, J. A. Briggs, S. G. Megason, and A. M. Klein, Single-cell mapping of gene expression landscapes and lineage in the zebrafish embryo, Science **360**, 981 (2018).

[5] H. Cheng, Z. Zheng, and T. Cheng, New paradigms on hematopoietic stem cell differentiation, Protein & Cell **11**, 34 (2020).

[6] S. Mani and T. Tlusty, A topological look into the evolution of developmental programs, Biophys. J. **120**, 4193 (2021).

[7] S. Ruijtenberg and S. van den Heuvel, Coordinating cell proliferation and differentiation: Antagonism between cell cycle regulators and cell type-specific gene expression, Cell Cycle **15**, 196 (2016).

[8] C. Waddington, *The Strategy of the Genes* (George Allen & Unwin LTD, London, 1957), p. 274.

[9] S. A. Kauffman, Metabolic stability and epigenesis in randomly constructed genetic nets, J. Theor. Biol. **22**, 437 (1969).

[10] J. Wang, L. Xu, and E. Wang, Potential landscape and flux framework of nonequilibrium networks: Robustness, dissipation, and coherence of biochemical oscillations, Proc. Natl. Acad. Sci. USA **105**, 12271 (2008).

[11] C. Furusawa and K. Kaneko, Emergence of rules in cell society: Differentiation, hierarchy, and stability, Bull. Math. Biol. **60**, 659 (1998).

[12] C. Furusawa and K. Kaneko, Theory of robustness of irreversible differentiation in a stem cell system: Chaos hypothesis, J. Theor. Biol. **209**, 395 (2001).

[13] C. Furusawa and K. Kaneko, A dynamical-systems view of stem cell biology, Science **338**, 215 (2012).

[14] R. J. De Boer and A. S. Perelson, Quantifying T lymphocyte turnover, J. Theor. Biol. **327**, 45 (2013).

[15] See Supplemental Material at http://link.aps.org/supplemental/10.1103/PhysRevResearch.5.L022052 for the derivation of equations, and mathematical and biological details, which includes Refs. [30–35].

[16] L. Ambrosio, N. Gigli, and G. Savaré, *Gradient Flows in Metric Spaces and in the Space of Probability Measures* (Birkhäuser, Basel, 2005), p. 334.

[17] A. Mielke, A gradient structure for reaction-diffusion systems and for energy-drift-diffusion systems, Nonlinearity **24**, 1329 (2011).

[18] A. Mielke, M. A. Peletier, and D. R. M. Renger, On the relation between gradient flows and the large-deviation principle, with applications to Markov chains and diffusion, Potential Anal. **41**, 1293 (2014).

[19] R. J. De Boer and A. S. Perelson, Towards a general function describing T cell proliferation, J. Theor. Biol. **175**, 567 (1995).

[20] R. Antia, C. T. Bergstorm, S. S. Pilyugin, S. M. Kaech, and R. Ahmed, Models of CD8+ responses: 1. What is the antigen-independent proliferation program, J. Theor. Biol. **221**, 585 (2003).

[21] A. J. Anelone and S. K. Spurgeon, Modelling and simulation of the dynamics of the antigen-specific T cell response using variable structure control theory, PLoS One **11**, e0166163 (2016).

[22] R. J. De Boer, M. Oprea, R. Antia, K. Murali-Krishna, R. Ahmed, and A. S. Perelson, Recruitment times, proliferation, and apoptosis rates during the CD8+ T-cell response to lymphocytic choriomeningitis virus, J. Virol. **75**, 10663 (2001).

[23] I. den Braber, T. Mugwagwa, N. Vrisekoop, L. Westera, R. Mögling, A. Bregje de Boer, N. Willems, E. Schrijver, G. Spierenburg, K. Gaiser, E. Mul, S. Otto, A. Ruiter, M. Ackermans, F. Miedema, J. Borghans, R. de Boer, and K. Tesselaar, Maintenance of peripheral naive T cells is sustained by thymus output in mice but not humans, Immunity **36**, 288 (2012).

[24] T. J. Kobayashi, D. Loutchko, A. Kamimura, and Y. Sughiyama, Kinetic derivation of the Hessian geometric structure in chemical reaction networks, Phys. Rev. Res. **4**, 033066 (2022).

[25] N. Ab Azar, A. Shahmansoorian, and M. Davoudi, From inverse optimal control to inverse reinforcement learning: A historical review, Annu. Rev. Control **50**, 119 (2020).

[26] P. Zhou, S. Wang, T. Li, and Q. Nie, Dissecting transition cells from single-cell transcriptome data through multiscale stochastic dynamics, Nat. Commun. **12**, 5609 (2021).

[27] R. C. Kraaij, A. Lazarescu, C. Maes, and M. Peletier, Fluctuation symmetry leads to GENERIC equations with non-quadratic dissipation, Stochastic Processes Appl. **130**, 139 (2020).

[28] T. J. Kobayashi, D. Loutchko, A. Kamimura, and Y. Sughiyama, Hessian geometry of nonequilibrium chemical reaction networks and entropy production decompositions, Phys. Rev. Res. **4**, 033208 (2022).

[29] M. A. Peletier, Variational modelling: Energies, gradient flows, and large deviations, arXiv:1402.1990.

[30] J. Dolbeault, B. Nazaret, and G. Savaré, A new class of transport distances between measures, Calc. Var. Partial Differ. Equations **34**, 193 (2009).

[31] M. Liero, A. Mielke, and G. Savaré, Optimal transport in competition with reaction: The Hellinger–Kantorovich distance and geodesic curves, SIAM J. Math. Anal. **48**, 2869 (2016).

[32] S. Kondratyev, L. Monsaingeon, and D. Vorotnikov, A new optimal transport distance on the space of finite radon measures, Adv. Differential Equations **21**, 1117 (2016).

[33] L. Chizat, G. Peyré, B. Schmitzer, and F.-X. Vialard, An interpolating distance between optimal transport and Fisher-Rao metrics, Found. Comput. Math. **18**, 1 (2018).

[34] A. Esposito, F. S. Patacchini, A. Schlichting, and D. Slepčev, Nonlocal-interaction equation on graphs: Gradient flow structure and continuum limit, Arch. Ration. Mech. Anal. **240**, 699 (2021).

[35] D. Homann, L. Teyton, and M. B. A. Oldstone, Differential regulation of antiviral T-cell immunity results in stable CD8+ but declining CD4+ T-cell memory, Nat. Med. **7**, 913 (2001).